EXAFS studies of aqueous solutions of manganese(II) chloride and bromide: structural

variations with concentration and interactions with solvent

EXAFS studies of aqueous solutions of manganese(II) chloride and bromide: structural variations with concentration and interactions with solvent

B Beagley†, C A McAuliffe, S P B Smith and E W White

Department of Chemistry, University of Manchester Institute of Science and Technology, PO Box 88, Manchester M60 1QD, UK

Abstract. EXAFS data, collected at the SRS at Daresbury Laboratory, for aqueous solutions of $MnBr_2$ and $MnCl_2$ at a variety of concentrations were analysed by least-squares curve fitting calculations. The data, obtained at ambient temperature, were found to be consistent with equilibria between species of the type $[MnX_{(6-n)}(H_2O)_n]^{(n-4)+}$ (where X = Cl, Br and $n = 4, 5, 6$) for which it was possible to determine the average value of n (i.e. n_{av}) at each concentration. To fit the data, a third distance, in addition to Mn–X and Mn–O in the complexes, was shown to be significant in the least-squares calculations; this third distance at 4.4 Å represents the radius of the first hydration sphere around the complexes and is reasonably interpreted as Mn to solvent water molecules hydrogen bonded to the water molecules in the complexes. By carefully parameterising the calculations using EXAFS data for solid reference compounds, the dependence of n_{av} on concentration was determined; calculations were carried out both with data sets for single concentrations and also with data sets for four different concentrations simultaneously. The latter calculations enabled the direct refinement of the slope k and the intercept M_0 for the concentration dependence represented as $n_{av} = M_0 - kc/\text{mol dm}^{-3}$, where c is the concentration. For both $MnCl_2$ and $MnBr_2$ solutions, M_0, the number of water ligands in the complex at infinite dilution, was found to be 6, as expected. The slopes k were found to be 0.18(1) and 0.25(1), respectively. The greater slope in the case of $MnBr_2$ shows that its solutions have a smaller value of n_{av} than found in comparable $MnCl_2$ solutions; in neither case does n_{av} reach 4 before saturation occurs.

1. Introduction

Previous EXAFS (extended x-ray absorption fine structure) studies of aqueous $MnBr_2$ solutions [1] showed the presence of Mn–Br bonds in concentrated samples and interpreted the changing behaviour with concentration in terms of variations in the equilibrium mixture of species $[MnBr_{(6-n)}(H_2O)_n]^{(n-4)+}$, $n = 4, 5, 6$ with concentration [2]. A linear relationship between the average value of n ($=n_{av}$) was found to fit the observations, although the value of n_{av} at infinite dilution, unexpectedly, did not appear to extrapolate to 6. The present work extends these studies to aqueous $MnCl_2$ solutions and, by more careful avoidance of correlation between the structural parameters in the

† Author to whom correspondence should be addressed.

least-square curve-fitting calculations, shows that the data fit a regime in which the value of n_{av} at infinite dilution is 6 for both $MnCl_2$ and $MnBr_2$ solutions.

The present work also extends previous studies [3] of the interaction of the complexes with the solvent water molecules, by obtaining more accurate values for the radius of the first sphere of solvent water molecules around the manganese(II) atoms in both halide solutions.

2. Experimental details and method

EXAFS data for the solutions were collected at room temperature on beamline 7.1 at the Synchrotron Radiation Source (SRS) at Daresbury Laboratory, UK, using a variety of solution cells. Solid samples were checked for phase purity at UMIST by x-ray powder diffraction; at Daresbury they were ground to a fine powder and deposited on sticky tape. The majority of the data used in the calculations reported here were collected in the early years of the SRS with an electron beam current of 1.8 GeV and a typical stored current of 200 mA. All the spectra were recorded at the manganese K-edge (1.90 Å, 6.54 keV), but over a period of time both transmission and fluorescence detection [4] were used and both types of monochromatisation were available: Si(220) with harmonic rejection (usually 50%) [5] and Si(111) with and without double focusing mirror. Ion chambers containing argon and helium mixed in the proportions recommended at the SRS for the manganese K-edge were used for reference in the fluorescence mode and for both reference and sample counts in the transmission mode. Energy calibration was achieved by using a manganese foil and setting the monochromator-position recorder to deliver the tabulated value for the edge energy at the mid-point of the edge. Our studies of the solutions produced consistent EXAFS spectra for given concentrations regardless of experimental conditions.

The raw EXAFS data were processed to background subtracted χ-curves using the programs EXCALIB and EXBACK in the Daresbury program library and the χ-curves were transferred to the Manchester Computing Centre (MCC) via the academic computer network administered by a Prime computer at UMIST. Subsequent calculations were performed on the MCC's Amdahl 5890-300 by means of the VM/CMS facilities (virtual machine/conversational monitor system). The least-squares curve fitting calculations employed the UMIST software [3], using the plane-wave approximation and careful calibration with reference compounds, to take advantage of the superior flexibility of the software over other systems (see below).

The form of the equation [3 and references therein] used by the UMIST software is, for the K-edge of x-ray absorber element a:

$$\chi(k) = -\sum_{b}[M_b/k(R_{ab})^2]|f_b(k,\pi)|\sin[2k(R_{ab}-\Delta R_{ab})+2\varphi_a(k)+\varphi_b(k)]$$

$$\times \exp[-2k^2(\sigma_{ab})^2 - 2R_{ab}\eta/k - \theta]$$

where the summation is over all back-scattering atoms b, M_b is the number or multiplicity of atoms of type b, R_{ab} is the distance a–b, ΔR_{ab} is a correction to the distance to compensate for phase-shift deficiencies, $(\sigma_{ab})^2$ is a Debye–Waller term made up of two contributions $(U_{ab})^2 + (\sigma_{dis})^2$, with U_{ab} the normal spectroscopic root mean square vibrational amplitude for R_{ab} and σ_{dis} is a disorder parameter, of particular importance e.g. when averaging over bonds of a given type a–b which are not equal in length.

Table 1. Typical results from refinements for solid reference compounds, providing calibration parameters for calculations with data for manganese(II) halide solutions.[a] Distances R, phase parameters ΔR, and vibrational amplitudes U in Å (1 Å = 10^{-10} m). M are the multiplicities of the distances in the complexes. EXAFS data ranges in Hartree (1 Hartree = 27.2 eV). ESD in the last figure quoted are given in parentheses; f = fixed at value from literature.

Solid	Manganese(II) Tutton's salt[b]	Manganese(II) perchlorate[c]	[MnCl$_2$(H$_2$O)$_4$] solid[d]	[MnBr$_2$(H$_2$O)$_4$] solid[e]	Average[f]
Ref.	[6]	[7]	[8]	[9]	
R_1	2.18(f)	2.18(f)	2.20(f)	2.18(f)	
ΔR_1	0.32(1)	0.34(1)	0.32(1)	0.31(1)	(Cl)0.33
U_1	0.113(1)	0.112(1)	0.106(2)	0.107(1)	(Br)0.31
M_1	6.00(f)	6.00(f)	4.00(f)	4.00(f)	0.111
R_2	—	—	2.49(f)	2.64(f)	
ΔR_2	—	—	0.33(1)	0.25(1)	(Cl)0.31
U_2	—	—	0.089(1)	0.101(1)	(Br)0.24
M_2	—	—	2.00(f)	2.00(f)	(Cl)0.089
Res[g]	0.062	0.083	0.09	0.14	(Br)0.100
Data range	2.5–15.0	2.5–15.0	2.5–15.0	2.5–15.0	

[a] Subscripts: 1 refers to Mn–O distances; 2 refers to Mn–X distances, X = Cl, Br. Longer distances were fixed at literature values (see below).

[b] [Mn(H$_2$O)$_6$](NH$_4$)$_2$(SO$_4$)$_2$; calculations included longer distances to O at 4.33(1), and to S at 4.90(f).

[c] [Mn(H$_2$O)$_6$](ClO$_4$)$_2$; calculations included longer distances to O at 4.48(1), to Cl at 4.96(1) and to Mn at 5.27(f).

[d] Calculations included longer distances to O at 4.37(1) and to Cl at 4.77(1).

[e] Calculations included longer distances to O at 4.52(1) and to Br at 4.71(1).

[f] Calibration values; (Cl) or (Br) refer to the values appropriate for MnCl$_2$ or MnBr$_2$ solutions. The averages quoted are a consensus of values from calculations on several samples of the appropriate solid reference compounds (for tests of these consensus values, see table 2).

[g] The conventional residual (sum of $\Delta\chi$/sum of χ_{expt}), where $\Delta\chi = \chi_{expt} - \chi_{calc}$.

Amplitude $|f_b(k, \pi)|$ and angle $\varphi_b(k)$ are the amplitude and phase of the photo-electron back-scattering factor, where k is the photo-electron wave vector, $\varphi_a(k)$ is the phase shift associated with the absorber atom, η is the principal mean path parameter arising from inelastic scattering (fixed at 1.5 Å^{-2} throughout this work) and θ represents lesser free path terms, normally taken as zero in the EXAFS region. The scattering amplitudes and phases are calculated from particle wave phases δ_ℓ obtained from the Daresbury computer library. Multiplicity is not the same as the chemical coordination number, which is the total multiplicity for atoms chemically bonded to the absorber; in this work with both Mn–O and Mn–X bonds present (X = Cl or Br), the coordination number is constant, being six in each of the complexes present in the solution equilibria.

3. Structure determination

3.1. Reference compounds

Calculations using EXAFS data from solid compounds are particularly important in the

Table 2. Results obtained on checking the calibration parameters[a] by refining multiplicities in reference compounds. Parameter labelling, etc., and inclusion of longer distances, as in table 1.

	$[MnCl_2(H_2O)_4]$ solid	'Consensus' values[b]	$[MnBr_2(H_2O)_4]$ solid	'Consensus' values[b]
R_1	2.20(f)		2.18(f)	
U_1	0.110(2)	0.111	0.111(f)	0.111
M_1	4.3(2)		4.07(5)	
ΔR_1	0.34(2)	0.33	0.30(1)	0.31
R_2	2.49(f)		2.64(f)	
U_2	0.083(4)	0.089	0.100(f)	0.100
M_2	$6.00\text{-}M_1$		$6.00\text{-}M_1$	
ΔR_2	0.32(1)	0.31	0.25(1)	0.24
Res.	0.09		0.14	

[a] Correlations bigger than ± 0.9 occur between parameters such as U_1, M_1, ΔR_1, U_2, and ΔR_2 in calculations of this type; thus later calculations on solutions employ the 'consensus' values to avoid destabilising the refinements. Note, e.g., that it was necessary to fix U_1 and U_2 in the above calculations for the bromide to avoid such destabilisation.

[b] Calibration parameters averaged from calculations on many samples (see table 1).

present studies, because the simultaneous presence of Mn–O and Mn–X (X = Cl, Br) bonds in the aqueous solutions gives rise to serious parameter correlation problems (see below). Four solid reference compounds of known crystal structure were employed. The first two reference materials contain the hexa-aquo complex $[Mn(H_2O)_6]^{2+}$; these are the manganese Tutton's salt [6], $[Mn(H_2O)_6](NH_4)_2(SO_4)_2$, and manganese perchlorate hexahydrate [7], $[Mn(H_2O)_6](ClO_4)_2$. The others are the solid tetrahydrates of the relevant halides; crystal structure determinations of these have shown the presence of discrete units of the hydrated complexes $[MnX_2(H_2O)_4]$ where X = Cl, Br and X ligands are *cis* [8, 9], although in solution, *cis* and *trans* forms of this non-ionic species may be present.

As EXAFS studies measure short range order associated with the molecular complexes, and it can be assumed (in the present case) that the molecular complexes present are similar geometrically in solid and aqueous phases, then bond lengths R, measured crystallographically, can be carried over to EXAFS studies of solids or solutions to within the reproducibility of the EXAFS results (with ESD of say ± 0.01 Å). The EXAFS phase parameters ΔR, which depend largely on the nature of absorber and backscatterer, are thus likewise transferable from solid to solution for a given back-scatterer. Vibrational amplitudes U, given the similar geometrical environment, will also be transferable. Our own experience [10] with solid manganese(II) perchlorate and the manganese(II) Tutton's salt and their aqueous solutions has confirmed this. (Transferring crystallographically determined Debye–Waller parameters is not valid, because the latter include contributions from lattice vibrations; such transfers are not attempted.)

In determining calibration parameters for use in calculations using EXAFS data for the aqueous solutions, structural parameters from the crystallographic results were held constant at the literature values, while vibrational and phase parameters were refined by full-matrix least-squares curve fitting. Typical results from these refinements are given in table 1. Also given are the averaged values of the refined calibration parameters,

obtained from a consensus of a wide range of calculations on several samples of each of the reference materials.

To check the suitability of the values intended for use in the studies of the solutions, further calculations on the tetrahydrate solids were carried out with the multiplicity M_1 for the Mn–O bonds refined, and that for the Mn–X (X = Cl, Br) bonds constrained during the refinement at $M_2 = 6.00 - M_1$, using a standard feature of the flexible software. The results are shown in table 2. Table 2 shows that refining the Mn–O bond multiplicity gives $M_1 = 4.00$ within 1–2 ESD and the other refined parameters remain at the 'consensus' values, with the same margin; these calculations give confidence that, at least in the cases where M_2 (=2, here) is significant, the calibration parameters are satisfactory and refinement of M_1 leads to the correct result.

Latham *et al* [11] have addressed the problem of detecting mixed back-scattering from Zn–O and Zn–X bonds in dried polymer:ZnX₂ films, however they apparently did not feel able to use the constraint $M_2 = 6.00 - M_1$ for such materials. Consequently, they had difficulty in obtaining good values for M_1 and M_2 although they clearly demonstrated that both types of back-scatterer are present. They added that the effect of the oxygen back-scatterer is more clearly seen in the presence of Cl than with Br or I. The present use of the constraint and the 'consensus' values for U and ΔR parameters allows curve fitting with solution data, below, to converge more effectively. In the present work, preliminary calculations on the MnCl₂ (but not with MnBr₂) solutions tended to over-emphasize the contribution from Mn–X bonds, a finding which is not quite what Latham *et al* reported about lighter halides; but the origin of these effects with the lighter halogen is likely to be associated with the fact that metal-to-X bond lengths are less different from metal-to-O bond lengths when X is the lighter halogen, so that parameter correlation problems are more severe in such cases. Thus the present approach leans heavily on the use of known data from other sources (e.g. from the reference compounds) to overcome such ambiguities. The 'consensus' value of 0.111 Å for U_1 (for Mn–O) can be compared with the observed values from x-ray diffraction studies of MnSO₄ solutions of 0.10(2) [12], 0.104(5) [13] and also the higher value of 0.132(2) Å [14] in Mn(NO₃)₂ solution where disorder of Mn–O distances is present in the form of Mn to nitrate-oxygen and water–oxygen bonding. The 'consensus' value of 0.100 Å for U_2 for Mn–Br is not unreasonable when compared with the value of 0.086(2) Å observed by gas-phase electron diffraction for a much stronger, and 0.3 Å shorter, Mn–Br bond in monomeric MnBr₂ [15].

3.2. Interaction with solvent

Turning to the EXAFS data collected for aqueous solutions of MnBr₂, it is clear from the earlier work [2, 3] that an M_1 value of a little less than 5, with M_2 about 1, is obtained for saturated solutions. This suggests that (on average) each Mn atom in saturated solution has about one X atom bonded to it in the mixture of species $[\text{MnBr}_{(6-n)}(\text{H}_2\text{O})_n]^{(n-4)+}$, with $n = 4, 5, 6$. In view of the test calculations of table 2, the most reliable calculations on the solutions are arguably these for the saturated solutions, which have the largest values of M_2 (about 1) obtained in calculations on solutions.

Least-squares curve fitting calculations with many sets of EXAFS data for saturated MnX₂ (X = Cl, Br) solutions have been performed. Basing these calculations on contributions from Mn–O and Mn–X bonds *only* has never given a good fit between calculation and experiment, regardless of whether the 'consensus' calibration par-
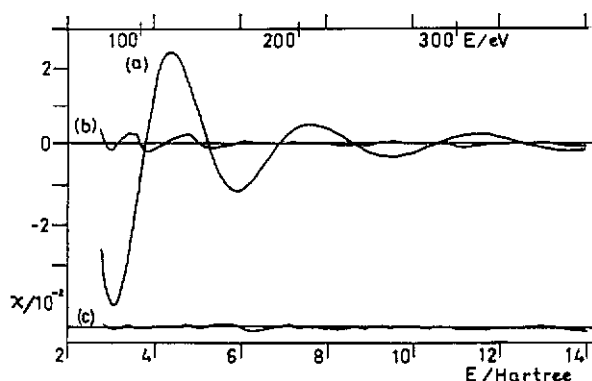
Figure 1. EXAFS curves for 4.95 mol dm^{-3} MnCl$_2$ solution. (a) Experimental χ-curve; (b) curve (a) with calculated contributions for Mn–O and Mn–Cl bonds subtracted; (c) as (b), but contribution for Mn . . . O(solvent) also subtracted.

ameters were fixed or given freedom to vary. The misfit which results is illustrated in figure 1. After the contributions from the Mn–O and Mn–X bond distances have been subtracted from the observed EXAFS curves there are always high-frequency ripples remaining in the data region out to about 6 Hartree (figure 1(*b*)) suggesting that a third and longer distance has so far been omitted from the calculations. The ripple frequency is about twice that of the main EXAFS features, suggesting a longer distance about twice that of the average of the Mn–O and Mn–X bond distances, namely about 4.5 Å.

Including a third distance eliminates the misfit. Figure 1(*c*) is the resulting difference curve with the contribution of this third distance also subtracted. The numerical results suggest that back-scattering from about 10–20 solvent oxygen atoms accounts for the ripples in figure 1(*b*); the refined values of Mn . . . O distances obtained in a series of refinements were about 4.4 Å. Details will be given below.

We have also observed such Mn . . . O(solvent) contributions in aqueous solutions of manganese(II) nitrate [3], perchlorate and the Tutton's salt [10], and in solutions of other first-row transition metal salts [16]. We have carried out statistical tests, e.g. the special tests for judging the significance of an added distance [17]; in all cases where good quality data were available, confirmation was obtained that inclusion of the Mn . . .O(solvent) distance significantly improves the least-squares fit between observed and calculated EXAFS curves. X-ray diffraction studies of aqueous solutions of other manganese(II) salts have also led to reports of Mn . . . O(solvent) distances with comparable values: in MnSO$_4$ solution, 4.34–4.35 [12] and 4.17(1) [13] and in Mn(NO$_3$)$_2$ solution, 4.25(1) Å [14]; variation with the nature of the anionic species is to be expected.

3.3. Variations with concentration

In the earlier work on aqueous solutions of MnBr$_2$, the variation with concentration of M_1 (i.e. the average value of n for the mixture of complexes present) was noted. However, at that time the significant effect of correlation between parameters, especially for the dilute solutions, was not fully appreciated. The consequence was that the slope of the variation of $n = n_{av}$ with concentration was underestimated. Our later work on both MnBr$_2$ and MnCl$_2$ solutions has shown that the data are compatible with an intercept of $n_{av} = 6.0$ at infinite dilution, which is in keeping with thermodynamic expectations (e.g. inferred from equation (3.18) in [18]). The work leading to this conclusion will now be presented.
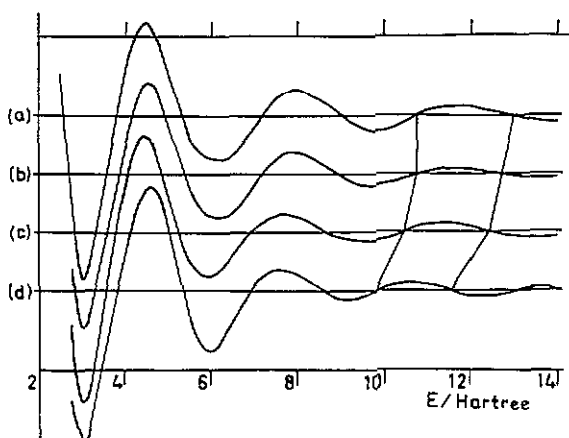
Figure 2. Experimental EXAFS curves for various solutions. 'Vertical' lines show movement of cross-over points to the *left* denoting *increasing* average Mn–X distance through the series. (a) Mn(ClO₄)₂ solution; (b) dilute MnBr₂ solution (1.6 mol dm⁻³); (c) strong MnCl₂ solution (4.95 mol dm⁻³); (d) strong MnBr₂ solution (5.2 mol dm⁻³).

In figure 2, a series of EXAFS curves is presented comparing data for some manganese(II) halide solutions with data for an aqueous solution of manganese(II) perchlorate, where the manganese(II) complex is known to be $[Mn(H_2O)_6]^{2+}$ [7]; as noted in table 1 the Mn–O distance in this complex in crystalline manganese(II) perchlorate hexahydrate is 2.18(1) Å [7] and EXAFS studies of its aqueous solution [10] are consistent with the value being the same in solution. Figure 2 shows a steady contraction of the EXAFS ripples towards the absorption edge through the series of solutions; to emphasize this, lines have been drawn joining corresponding cross-over points for each solution. The contraction of the ripples towards the origin implies a gradual increase in the average bond length in the series of solutions. The curves show that the longest average distance is for saturated MnBr₂ solution (average of Mn–O and Mn–Br), while the dilute MnBr₂ solution has an average distance nearer to that in the hexahydrate complex; the dilute solution clearly has a larger ratio of Mn–O bonds to Mn–Br bonds (i.e. n_{av} is larger for the dilute solution). In the case of saturated MnCl₂ solution, the intermediate average distance is affected not only by the ratio of Mn–O to Mn–Cl bonds, but also by the fact that Mn–Cl bonds are shorter than Mn–Br bonds. The observed closer similarity of the curves for saturated MnCl₂ and $[Mn(H_2O)_6]^{2+}$, due to these factors, suggests that the problem of resolving the dependence of n_{av} on concentration is more difficult in the case of the MnCl₂ solutions than in the case of the MnBr₂ solutions.

Although we achieved a degree of success in our earlier work on MnBr₂ solutions in establishing the dependence of n_{av} on concentration, we have already noted the difficulties, even for MnBr₂ solutions, when working with samples of low concentration. This suggests even greater problems for MnCl₂ solutions arising from parameter correlation; hence, the need to establish, as described above, a suitable set of calibration parameters is an essential, though time-consuming, exercise. In table 3, the results of least-squares curve fitting calculations on MnCl₂ solutions are presented in which the calibration parameters are held fixed at their 'consensus' values. In view of the large number of calculations performed for reference compounds, and the testing of these fixed 'consensus' values (e.g. see table 2), these can confidently be carried over to the calculations for the solutions. As the values shown in table 3 for $M_1 = n_{av}$ indicate, this procedure demonstrates the expected increase in n_{av} with dilution, however the error level is still such that the values of n_{av} obtained do not show a regular change with changing concentration. This irregularity in the curve of n_{av} versus concentration was

Table 3. Typical results from refinements for aqueous solutions of $MnCl_2$, carried out with the calibration parameters fixed at their 'consensus' values, showing the variation of M_1 ($= n_{av}$) with concentration c. Parameter labelling, etc., as in table 1; parameters for distance 3, Mn ... O(solvent) are included. Fixed parameters: $R_1 = 2.20$, $\Delta R_1 = 0.33$, $U_1 = 0.111$, $R_2 = 2.49$, $\Delta R_2 = 0.31$, $U_2 = 0.089$, $U_3 = 0.15$. Data ranges: 2.5–14.0 Hartree.

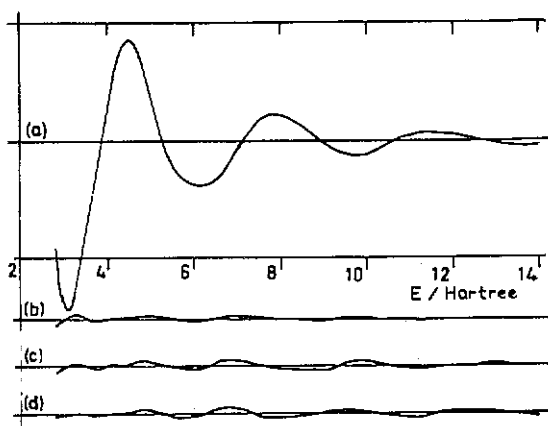| $c/\text{mol dm}^{-3}$	4.95	2.95	1.96	1.00	0.10
$M_1 = n_{av}$	5.3(1)	5.2(1)	5.7(1)	5.6(1)	6.0(2)
M_2	$6.0 - M_1$	$6.0 - M_1$	$6.0 - M_1$	$6.0 - M_1$	$6.0 - M_1$
R_3	4.43(1)	4.43(1)	4.42(1)	4.44(2)	4.43(2)
ΔR_3	$= \Delta R_1$	$= \Delta R_1$	$= \Delta R_1$	$= \Delta R_1$	$= \Delta R_1$
M_3	14(2)	17(2)	16(2)	18(1)	17(4)
Res.	0.074	0.066	0.103	0.15	0.18

Figure 3. EXAFS curves for 1.96 mol dm^{-3} $MnCl_2$ solution. (a) Experimental χ-curve; (b) curve (a) with calculated curve, based on parameters in table 3, subtracted; (c) as (b), showing poorer fit with M_1 fixed at 6, and U_1 and ΔR_1 refined instead (see text); (d) as (c), but for 4.95 mol dm^{-3} solution, showing poorer fit compared with curve (c) of figure 1.

also found in the earlier work on $MnBr_2$ solutions [2]; it is to be expected because of the difficulties in obtaining a precise value for n_{av} from a single data set. The goodness of fit between observed and calculated EXAFS is typified by the difference curve in figure 1(c). However, the conventional residual increases as the x-ray absorption data becomes increasingly noisy with dilution. To provide additional evidence that the curve fitting realistically gives n_{av}-values less than 6 (table 3), figure 3 is presented, which shows that poorer fits are obtained in calculations where n_{av} is fixed at 6 (no Mn–X bonds present); results are presented for $c = 1.96$ and 4.95 mol dm^{-3} $MnCl_2$ solutions. In these calculations with n_{av} fixed, U_1 and ΔR_1 were refined instead; values of 0.110(1) and 0.114(1) Å for U_1, and 0.32(1) and 0.30(1) Å for ΔR_1 were obtained, respectively, for the two concentrations. Although one extra variable is thus included in these calculations the fits are poorer, showing that omitting the Mn–Cl bonds from the curve fitting worsens the fits; similar results are obtained from calculations with $MnBr_2$ solutions.

With the UMIST least-squares curve fitting program [3] it is routinely possible to use data from several experiments simultaneously. Furthermore, the user can select for refinement parameters associated with any aspect of the curve fitting methodology. To obtain a direct measure of the variation of n_{av} with concentration, four data sets

Table 4. The results of composite refinements for aqueous solutions of MnCl$_2$, using four data sets simultaneously, to obtain the dependence of n_{av} on concentration c, assuming M_1(calc.) $= M_0 - kc/$mol dm^{-3}. Parameter labelling, etc., as in table 1; parameters for distance 3, Mn . . . O(solvent) are included. Refined M_1 values from table 3 are given for comparison. Fixed parameters: $R_1 = 2.20$, $\Delta R_1 = 0.33$, $U_1 = 0.111$, $R_2 = 2.49$, $\Delta R_2 = 0.31$, $U_2 = 0.089$, $U_3 = 0.15$. Data ranges: 2.5–14.0 Hartree.

$c/$mol dm^{-3}	4.95	2.95	1.00	0.10
M_1(table 3)	5.3(1)	5.2(1)	5.6(1)	6.0(2)
k refined with M_0 fixed:				
	slope, $k = 0.18(1)$;		intercept, $M_0 = 6.0(f)$	
M_1(calc.)	5.1	5.5	5.8	6.0
M_2	$6.0 - M_1$	$6.0 - M_1$	$6.0 - M_1$	$6.0 - M_1$
	$R_3 = 4.42(1)$;		$\Delta R_3 = \Delta R_1$	
	$M_3 = 17(1)$;		Res. = 0.13	
k and M_0 refined:				
	slope, $k = 0.15(1)$;		intercept, $M_0 = 5.9(1)$	
M_1(calc.)	5.2	5.5	5.75	5.9
M_2	$6.0 - M_1$	$6.0 - M_1$	$6.0 - M_1$	$6.0 - M_1$
	$R_3 = 4.43(1)$;		$\Delta R_3 = \Delta R_1$	
	$M_3 = 17(1)$;		Res. = 0.13	

representing four different concentrations were simultaneously included in a least-squares curve fitting calculation. The problems of parameter correlation are such that it is realistic to assume the simplest form of relationship between n_{av} and concentration c, namely linear, i.e.

$$n_{av} = M_0 - kc/\text{mol dm}^{-3}$$

where M_0 is the multiplicity at infinite dilution (the intercept of the function at $c = 0$) and k is a constant, the slope of the function. In effect, the least-squares calculations with four of the five data sets of table 3 were repeated in a single composite calculation, with k refined instead of the individual values of M_1. A further calculation with M_0 refined as well as k was performed; the results of both calculations are given in table 4. Similar calculations were performed using four data sets for MnBr$_2$ solutions, taken from the earlier work [2]. The corresponding results obtained for MnBr$_2$ solutions were $k = 0.25(1)$ with M_0 fixed at 6.0, and when M_0 was refined: $k = 0.24(1)$, $M_0 = 5.9(1)$. In both these calculations for MnBr$_2$, R_3 refined to 4.36(1) Å and M_3 to 13(1). The calculated values of M_1 (see table 4) are all within 3 ESD of the independently refined values in table 3.

4. Discussion

4.1. Interaction with solvent

With all the solution data, it was found necessary to include R_3, attributable to Mn . . . O(solvent), in the calculations, as has been demonstrated. The mean value of R_3 from the composite refinements for MnCl$_2$ (table 3) and MnBr$_2$ solutions, with M_0
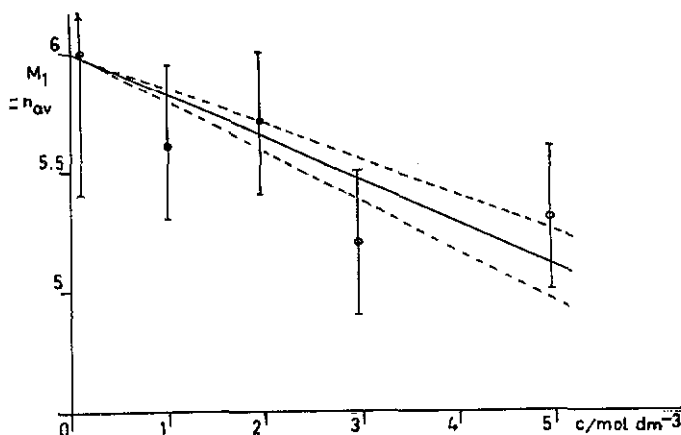
Figure 4. Relationship between average coordination number for oxygen, n_{av}, and concentration, c, for $MnCl_2$ solutions. Open circles show experimental points (from table 3) with error bars equal to 3 ESD. The full line is the fit obtained by calculations with multiple data sets (see table 4) and $M_0 = 6$; broken lines show 3 ESD limits.

fixed at 6.0, is close to 4.4 Å. This distance represents the radius of the first hydration sphere of solvent molecules around the Mn atom.

In the solid tetrahydrates of $MnCl_2$ [8] and $MnBr_2$ [9] there are Mn . . . O distances between adjacent $[MnX_2(H_2O)_4]$ complexes of 4.26 and 4.38 Å (average for the nearest three O atoms, in each case); these short contacts occur because the water molecules of adjacent complexes are linked by hydrogen bonds. It is reasonable to assume that in solution the complexes $[MnBr_{(6-n)}(H_2O)_n]^{(n-4)+}$ are hydrogen bonded to solvent water molecules in the first hydration sphere, giving rise to the Mn . . . O(solvent) distances at about 4.4 Å. The angle <Mn–O . . . O(solvent) can be calculated from this distance, the Mn–O distance of about 2.2 Å, and an assumed H-bond distance of about 2.7 Å, using the cosine rule, to be 127°. This is not an unreasonable angle for such a system, and is in agreement with data from the x-ray diffraction studies mentioned above, where the H-bond distance was found to be 2.73–2.78 [12, 13] and 2.71 Å [14].

4.2. Variations with concentration

If it is accepted that at infinite dilution the only manganese(II) species present in the $MnCl_2$ and $MnBr_2$ solutions is $[Mn(H_2O)_6]^{2+}$ (i.e. $M_0 = 6$, exactly) then the refinements with M_0 fixed at 6 can be regarded as giving the most reliable results from the present work. Thus, for aqueous $MnCl_2$ solutions of concentration c:

$$n_{av} = 6 - 0.18\, c/\text{mol dm}^{-3}$$

and for $MnBr_2$ solutions:

$$n_{av} = 6 - 0.25\, c/\text{mol dm}^{-3}.$$

For the $MnCl_2$ solutions, this concentration dependence is shown in figure 4. Figure 4 also reveals the consistency of the results at the 3 ESD level and demonstrates how the special calculations with multiple data sets summarize the individual studies. The x-ray diffraction study of $Mn(NO_3)_2$ [14] found similar types of complexes as in the present work, with Mn bound through oxygen to nitrate; for a 4.4 mol dm^{-3} solution, $n_{av} =$

5.4(1). This permits the prediction of a concentration dependence for $Mn(NO_3)_2$ solution of

$$n_{av} = 6 - 0.14\, c/\text{mol dm}^{-3}.$$

Using the UMIST software [3], rather than EXCURVE [19] or other similar software packages, has the advantages (among others) that several data sets can be included in refinements simultaneously and that the user has control over the parameters which can be selected for refinement. In the present case, for example, M_2 was constrained always to be equal to $6 - M_1$ and the slope (and intercept) of the concentration dependence were selected for refinement. In this way, an ESD for the slopes, with a value of 0.01, was obtained directly for both the sets of $MnCl_2$ and $MnBr_2$ solutions; the difference Δk between the slopes for the different halides is 0.07, with an ESD of $\sqrt{2} \times 0.01 = 0.014$. This difference between the slopes is at a significance level of 5 ESD and thus it is highly significant statistically, so that the behaviour of $MnCl_2$ and $MnBr_2$ solutions can be considered different in terms of concentration dependence. The greater slope in the case of $MnBr_2$ shows that its solutions have a smaller value of n_{av} than found in $MnCl_2$ solutions of the same concentration. In both cases saturation occurs before n_{av} reaches 4, the value in the solid tetrahydrates $[MnX_2(H_2O)_4]$. Our strongest solutions were saturated, or near to saturation, in the ambient conditions of the EXAFS experiment, where some degree of heating by the x-ray beam is to be expected. It is not appropriate to discuss here the features of the solution equilibria which are different in the two cases; this will be left for a future opportunity.

Acknowledgments

References

[1] Beagley B, Gahan B, Greaves G N and McAuliffe C A 1983 *J. Chem. Soc., Chem. Commun.* 1265
[2] Beagley B, Gahan B, Greaves G N, McAuliffe C A and White E W 1985 *J. Chem. Soc., Chem. Commun.* 1804
[3] Beagley B 1988 *Stereochemical Applications of Gas-Phase Electron Diffraction. Methods in Stereochemical Analysis* ed I Hargittai and M Hargittai (New York: VCH) ch 13
[4] Hasnain S S, Quinn P D, Diakun G P, Wardell E M and Garner C D 1984 *J. Phys. E: Sci. Instrum.* **17** 40
[5] Greaves G N, Diakun G P, Quinn P D, Hart M and Siddons D P 1983 *Nucl. Instrum. Methods* **208** 335
[6] Montgomery H, Chastain R V and Lingafelter E C 1966 *Acta Crystallogr.* **20** 731
[7] Al-Farhan K A 1988 *PhD Thesis* UMIST, Manchester, UK
[8] El-Saffar Z M and Brown G M 1971 *Acta Crystallogr.* B **27** 66
   Baur W H 1965 *Inorg. Chem.* **4** 1840
   Zalkin A, Forrester J D and Templeton D H 1964 *Inorg. Chem.* **3** 529
[9] Sudarsanan K 1975 *Acta Crystallogr.* B **31** 2720 (note: errors in some bond lengths in this reference have been corrected for the present work.)
[10] Beagley B 1991 unpublished
[11] Latham R J, Linford R G and Schlindwein W S 1989 *Faraday Discuss. Chem. Soc.* **88** 103
[12] Licheri G, Paschina G, Piccaluga G and Pinna G 1984 *J. Chem. Phys.* **81** 6059
[13] Caminiti R, Marongiu G and Paschina G 1982 *Z. Naturforsch.* A **37** 581
[14] Caminiti R, Cucca P and Pintori T 1984 *Chem. Phys.* **88** 155

[15] Hargittai M, Hargittai I and Tremmel J 1981 *Chem. Phys. Lett.* **83** 207
[16] Usman K K 1987 *PhD. Thesis* UMIST, Manchester, UK
[17] Joyner R W, Martin K J and Meehan P 1987 *J. Phys. C: Solid State Phys.* **20** 4005
[18] Hartley F R, Burgess C and Alcock R M 1980 *Solution Equilibria* (New York: Wiley) p 57
[19] EXCURVE 1990, a program for EXAFS curve fitting, Daresbury Laboratory, UK